Title
Identification of yeast proteins necessary for cell-surface function of a potassium channel

Journal
Proceedings of the National Academy of Sciences of the United States of America, 104(46)

ISSN
0027-8424

Authors
Haass, Friederike A
Jonikas, Martin
Walter, Peter
et al.

Publication Date
2007-11-01

Peer reviewed

Biological Sciences
Cell Biology

Identification of yeast proteins necessary for cell surface function of a potassium channel

Friederike A. Haass[1,2], Martin Jonikas[3,4], Peter Walter[4], Jonathan S. Weissman[3], Yuh-Nung Jan[2,4], Lily Y. Jan[2,4], Maya Schuldiner[3]

Author affiliation: [1]Neuroscience graduate program, [2]Howard Hughes Medical Institute and Department of Physiology, [3]HHMI and Department of Cellular and Molecular Pharmacology, [4]HHMI and Department of Biochemistry and Biophysics; University of California San Francisco, San Francisco, CA 94158

Corresponding author: Maya Schuldiner, Department of Cellular and Molecular Pharmacology, Howard Hughes Medical Institute, University of California San Francisco, 1700 4th Street, Byers Hall, San Francisco, CA 94158-2330, USA. Tel.: +1 415 502 8089; Fax: +1 415 514 4140; Email: mschuldiner@cmp.ucsf.edu

Author contributions: FAH designed and performed research, analyzed data, wrote the paper; MJ and PW provided data and analysis on UPR; JSW contributed new reagents and analytic tools; Y-NJ and LYJ designed research, wrote the paper; MS designed research, analyzed data, wrote the paper.

Number of pages: 16
Number of figures: 5
Number of tables: 1
Supplemental information: Supplemental Methods, 3 tables, 1 figure

Word count: 5,489
Character count: 34,927 (with spaces)

Abbreviations: Kir channel - inwardly rectifying K^+ channel, Kir3.2 - the G-protein activated inwardly rectifying K^+ channel GIRK2, Kir* - Kir3.2S177W, ER - endoplasmic reticulum, GPI-AP – glycosylphosphatidylinositol anchored proteins, UPR - Unfolded Protein Response, YPAGR – rich, galactose media, YPAD – rich, dextrose media

Abstract

Inwardly rectifying potassium (Kir) channels form gates in the cell membrane that regulate the flow of K^+ ions into and out of the cell, thereby influencing the membrane potential and electrical signaling of many cell types including neurons and cardiomyocytes. Kir channel function depends on other cellular proteins that aid in folding of channel subunits, assembly into tetrameric complexes, trafficking of quality controlled channels to the plasma membrane, and regulation of channel activity at the cell surface. We used the yeast *Saccharomyces cerevisiae* as a model system to identify proteins necessary for the functional expression of a mammalian Kir channel at the cell surface. A screen of 376 yeast strains each lacking one non-essential protein localized to the early secretory pathway identified seven deletion strains in which functional expression of the Kir channel at the plasma membrane was impaired. Six deletions were of genes with known functions in trafficking and lipid biosynthesis (*sur4*Δ, *csg2*Δ, *erv14*Δ, *emp24*Δ, *erv25*Δ, *bst1*Δ) and one deletion was of an uncharacterized gene (*yil039w*Δ). We provide genetic and functional evidence that Yil039wp, a conserved, phosphoesterase domain-containing protein, which we named **T**rafficking of **E**mp24p/Erv25p-dependent cargo **D**isrupted 1 (Ted1p), acts together with Emp24p/Erv25p in cargo exit from the ER. The seven yeast proteins identified in our screen likely impact Kir channel functional expression at the level of vesicle budding from the ER and/or the local lipid environment at the plasma membrane.

Introduction

Inwardly rectifying potassium (Kir) channels serve important physiological functions by regulating the membrane potential of many cell types including neurons, cardiomyocytes, kidney cells, and hormone secreting cells. Disruption of Kir channel function has been linked to human diseases such as periodic paralysis and neonatal diabetes (1).

Kir channel activity at the plasma membrane is influenced by the abundance of channels and by their functional properties. The number of channels at the cell surface is regulated at the level of channel transcription, biosynthesis, trafficking, and turnover (2). The functional properties of Kir channels are influenced by the membrane potential, local lipid environment, small molecules, and interacting proteins (3, 4). Structure-function studies have identified amino acid motifs and structural features of Kir channels involved in folding, assembly, and trafficking as well as in gating and selectivity (5-7). However, less is known about the cellular machinery that interacts with these motifs and allows Kir channels to reach the cell surface and function appropriately. We took advantage of the knowledge gained from structure-function studies of Kir channels and the genetic tools available in the yeast *Saccharomyces cerevisiae* to design a yeast screen aimed at identifying cellular proteins that play a role in Kir channel functional expression.

We chose to study Kir3.2, a mammalian G-protein activated inwardly rectifying K^+ channel, that can form homotetrameric channels and mediates inhibitory post-synaptic potentials in midbrain dopamine neurons (8). The mutation S177W (referred to as Kir*) renders Kir3.2 constitutively open in the absence of G-protein signaling, permeable to Na^+ as well as K^+, and does not disrupt functional expression of the channel at the cell surface of yeast or *Xenopus* oocytes (9, 10). Expression of mutated K^+ channels that are permeable to Na^+ overwhelms the Na^+ detoxification systems of yeast (11). Functional expression of Kir* can therefore be assayed based on growth inhibition, reflected by small yeast colony size, on media containing high Na^+ concentrations. We reasoned that growth inhibition conferred by Kir* could be overcome if channel biogenesis, trafficking, or function were disrupted.

The *Saccharomyces* Genome Deletion Project has generated a library of yeast strains each lacking one non-essential gene (12). Additional transgenes can be introduced

into the deletion strains using methods developed for Synthetic Genetic Array analysis (13, 14). We used these tools to introduce an inducible Kir* transgene into 376 yeast deletion strains each lacking an early secretory pathway-localized protein (15) and tested the resulting strains for growth inhibition on high Na^+ media conferred by Kir*. We identified seven yeast deletion strains with reduced growth inhibition on high Na^+ media, indicating that the strains are missing a gene involved in Kir* functional expression.

Results

Kir* slows yeast growth on high Na^+ media.

Kir3.2S177W tagged with GFP at the C-terminus (referred to as Kir*) was integrated into the genome of yeast (BY4742 background) under the control of a galactose inducible/ dextrose repressible promoter. Whereas yeast not carrying Kir* doubled every 3 hours in YPAGR media containing 500 mM Na^+, expression of Kir* slowed the doubling time to 7 hours (Fig. 1A). The inhibition of yeast growth by Kir* was also observed on solid media containing 500 mM Na^+ (Fig. 1A). Integration of the channel into the yeast genome did not affect yeast growth when channel expression was repressed by dextrose (Fig. 1B) or under low sodium conditions (Fig. 1C). Growth on high Na^+ media of yeast expressing Kir* was rescued in the vicinity of a filter disk containing the Kir channel blocker barium (16) (supplemental Fig. S1), supporting the conclusion that growth inhibition conferred by Kir* was due to Na^+ influx through the channel.

Yeast screen

Using the mating and random spore selection scheme developed for Synthetic Genetic Array (SGA) analysis (13, 14), we introduced the genomically integrated copy of Kir* into 376 strains from the MATa (BY4741) yeast deletion library (12), each carrying a deletion of an early secretory pathway-localized protein (15) (see online Table S1 for a list of the deletions, Table S2 for the selection scheme). Growth of the deletion strains carrying Kir* was tested on high Na^+ media containing galactose to induce Kir* expression and, to account for strain specific growth differences, normalized to growth on high Na^+ media containing dextrose where Kir* expression was repressed. Most deletion

strains behaved like control (BY4741) yeast and showed growth inhibition on high Na^+ media when Kir* was expressed. However, several strains grew into large colonies even though Kir* expression was induced. Follow-up tests of the Na^+-tolerant strains in liquid culture identified seven yeast deletion strains (*sur4*Δ, *csg2*Δ, *erv14*Δ, *emp24*Δ, *erv25*Δ, *bst1*Δ, and *yil039w*Δ) that grew well under high Na^+, Kir*-inducing conditions.

Deletion strains resistant to growth inhibition by Kir*

The candidates fell into two categories (Table 1). First, enzymes involved in sphingolipid biosynthesis: Sur4p, which catalyzes the formation of very long chain fatty acids (17), and Csg2p, a regulatory subunit of the complex that attaches mannose to inositol phosphorylceramide (18). Second, proteins involved in cargo selection and vesicle budding during ER-Golgi trafficking: Erv14p, a protein required for packaging of specific cargo into COPII vesicles (19, 20); Emp24p and Erv25p, p24 proteins that form a complex involved in COPII vesicle budding and trafficking of GPI-anchored and soluble proteins (21); Bst1p, an enzyme that removes the acyl chain from GPI anchors thereby allowing GPI-anchored proteins to leave the ER (22, 23); Yil039wp, a conserved, metallophosphoesterase domain-containing protein, with previously unknown function.

To ensure correct identification of the deletions and to rule out differences in the genetic background, mutations in the transgene or influences of mating type, the seven candidate deletion strains were remade using PCR-mediated gene disruption in the BY4742 background and the phenotypes confirmed using growth assays in liquid culture and on agar plates. When Kir* expression was induced by galactose the seven deletion strains grew faster than the control strain in media containing high Na^+ (500 mM YPAGR) (Fig. 1A). The ability of the deletion strains to grow faster in high Na^+ media was not due to general Na^+ tolerance, because when Kir* expression was repressed by dextrose, the deletion strains grew at a similar rate or, in the case of *sur4*Δ and *yil039w*Δ, more slowly than the control strain in media containing high Na^+ (500 mM YPAD) (Fig. 1B). The deletions did not enhance the ability of the yeast to metabolize galactose, as shown by comparable or slower growth in galactose containing media under conditions of low Na^+ (YPAGR, ~30 mM Na^+) (Fig. 1C). Finally, Na^+ tolerance under Kir* inducing conditions was not explained by osmotolerance, because the deletion strains grew at

similar rates or more slowly than control yeast in hyperosmotic media containing 1 M sorbitol (data not shown).

Although the deletion strains expressing Kir* grew faster than the control strain expressing Kir* in 500 mM Na^+ YPAGR (Fig. 1A), they did not grow as fast as a control strain without genomic insertion of Kir*, likely because the deletions did not entirely abolish Kir* function at the plasma membrane. This would be expected for deletions affecting trafficking or quality control, which often employ backup pathways (24, 25). In addition, the Na^+ sensitivity (Fig. 1B) and slow growth in galactose media (Fig. 1C) of some of the strains (*sur4*Δ, *erv14*Δ, *bst1*Δ, *yil039W*Δ) may have contributed to the incomplete rescue, because for these strains even complete loss of the Kir* function would not have resulted in the same growth as control yeast not carrying Kir*.

Based on the result that reduced growth inhibition of the deletion strains is dependent on Kir* expression in the presence of high Na^+, we concluded that Kir* functional expression at the plasma membrane was disrupted in these strains. However, it was also possible that the membrane potential of the deletion strains was depolarized.

Hygromycin B sensitivity of deletion strains

Na^+ influx through Kir* is driven by the hyperpolarized membrane potential of yeast. Therefore, growth inhibition by high Na^+ would be reduced if the deletion strains had more depolarized membrane potentials than control yeast. The small size of yeast precludes electrophysiological measurements of their membrane potential, however, relative membrane potentials can be assayed based on uptake of lipophilic cations or sensitivity to the antibiotic hygromycin B (26-28). We therefore tested whether the seven deletion strains were hygromycin resistant, indicative of depolarization, compared to control yeast. To ensure that our assay would detect depolarization of the membrane potential, we tested the yeast strain *pma1-105*, which carries a mutation in the proton ATPase Pma1p and has previously been shown to be depolarized (28). Growth of the *pma1-105* strain was inhibited less by hygromycin B than growth of the corresponding control DBY745 strain (Fig. 2A). Comparing the deletion strains identified in our screen to the corresponding control BY4742 strain (Fig. 2B), the *sur4*Δ and *erv14*Δ strains were slightly less inhibited by hygromycin, indicating that they may be more depolarized.

Hygromycin resistance has been reported for *sur4*-mutant strains in the BWG1-7A genetic background (29). However, the differences in relative growth rates in our experiment were not statistically significant (Dunnett's test comparing BY4742 to each deletion strain, $p>0.05$). Because hygromycin B sensitivity cannot be calibrated in terms of absolute changes in membrane potential, we cannot rule out that the tendency towards hygromycin resistance in *sur4*Δ and *erv14*Δ strains accounted, at least in part, for the reduced growth inhibition by Na^+ influx through Kir*. The *csg2*Δ strain showed a tendency (but Dunnett's test $p>0.05$) towards increased hygromycin sensitivity and the *emp24*Δ, *erv25*Δ, *bst1*Δ, and *yil039w*Δ strains had comparable hygromycin sensitivity to the control strain, suggesting that depolarization did not account for the ability of these deletion strains to grow under high Na^+ conditions while expressing Kir*.

Impaired complementation of *trk1*Δ *trk2*Δ yeast by Kir3.2V188G

To corroborate that the seven deletions impaired functional expression of Kir* at the cell surface we employed an independent assay. Yeast lacking the K^+ transporters Trk1p and Trk2p are starved for K^+ and therefore grow slowly on Low Salt media supplemented with low concentrations (0.5 mM) of K^+ (30). Growth is rescued by expression of Kir3.2V188G, a constitutively active, K^+ selective Kir3.2 channel (9). If the deletions identified in our screen disrupted Kir channel trafficking or function, we predicted that rescue of *trk1*Δ *trk2*Δ yeast by Kir3.2V188G would be impaired in the deletion background. Indeed, Kir3.2V188G rescued growth on 0.5 mM K^+ media poorly or not at all when *trk1*Δ *trk2*Δ yeast carried a deletion of *SUR4*, *CSG2*, *EMP24*, *ERV25*, *BST1* or *YIL039W* (Fig. 3). These yeast strains grew well on Low Salt media supplemented with 100 mM K^+, where they did not depend on functional expression of Kir3.2V188G. The *erv14*Δ *trk1*Δ *trk2*Δ strain expressing Kir3.2V188G could not be tested in this assay, because the strain grew slowly on Low Salt plates even when supplemented with 100 mM K^+.

Kir* expression levels and localization in the deletion strains

The Na^+ tolerant phenotype, impaired rescue of *trk1*Δ *trk2*Δ yeast and the known functions of Sur4p, Csg2p, Erv14p, Emp24p, Erv25p, and Bst1p, suggested that the

deletions might have affected Kir channel maturation or trafficking. We therefore performed Western blot analysis on each of the strains to test whether the deletions altered total protein levels of Kir*. Similar amounts of Kir* were present in samples from yeast expressing Kir* in the control or deletion background (Fig. 4A).

Given comparable expression levels of Kir* in the deletion strains, we examined whether the deletions altered the subcellular localization of the channel. Yeast were grown in galactose containing media to induce Kir* expression, fixed and mounted for imaging of the GFP-tagged Kir*. Optical sections through the middle of yeast cells showed two rings of GFP fluorescence and sections through the periphery of the cells showed tubular distribution of the GFP-tagged channel (Fig. 4B). The pattern of Kir*-GFP fluorescence was typical of ER-localized proteins (31) even in the control strain. This was consistent with studies showing heavy ER localization of Kir3.2 in mammalian cells (32). Given the predominant ER localization of Kir* even in the control background, alterations in ER retention in the deletion strains could not be readily detected.

Deletion of *YIL039W* slows Gas1p trafficking

Six of the seven mutants identified by our screen had well-characterized functions impacting trafficking and lipid biosynthesis, which could explain their effects on Kir* channel functional expression (see Discussion). However, it was unclear how the uncharacterized, but conserved Yil039wp influenced Kir* activity. A previously published quantitative genetic interaction map suggested that Yil039wp acts together with Emp24p and Erv25p in mediating trafficking of cargo out of the ER. In this epistasis mini array profile (E-MAP), colony sizes for all double mutant combinations were used to assess genetic interactions between ~400 strains each carrying a deletion in an early secretory pathway gene. When strains were clustered based on the similarity in their patterns of genetic interactions, the *emp24*Δ and *erv25*Δ strains alongside *erp1*Δ were most similar to each other out of all 400 strains. This similarity was expected, because Emp24p, Erv25p, and Erp1p act together in a physical complex (33, 34). The next most similar, and therefore most functionally related gene was *YIL039W*. Moreover, the double mutants of *yil039w*Δ and *emp24*Δ or *erv25*Δ displayed buffering genetic interactions (Fig.

5A adapted from (15)), i.e. in the absence of Emp24p/Erv25p there was little additional fitness cost to losing Yil039wp. Buffering genetic interactions were also observed using a fluorescent reporter of Unfolded Protein Response-induction. Both *yil039w*Δ and *erv25*Δ yeast (*emp24*Δ was not assayed for technical reasons) showed UPR activation. Deletion of *YIL039W* and *ERV25* together did not exacerbate the phenotype to the extent expected for functionally unrelated genes (e.g. *ALG3*, *OST3*, and *SPC2*, Fig. 5B). These relationships indicate that Yil039wp functions in a concerted manner with Emp24p/Erv25p.

To directly test whether Yil039wp, Emp24p, and Erv25p share a common function, we investigated whether ER exit of the GPI-anchored protein Gas1p, which is delayed in *emp24*Δ and *erv25*Δ strains (33, 35), was affected in the yil*039w*Δ strain. Western blot analysis of whole cell extracts showed that Gas1p accumulated in its 100 kDa core-glycosylated ER form to a similar extent in yeast lacking EMP24, ERV25, or *YIL039W* (Fig. 5C). We therefore named *YIL039W* **T**rafficking of **E**mp24p/Erv25p-dependent cargo **D**isrupted 1 (*TED1*).

Discussion

Yeast has been used extensively as a model system to study K^+ channel structure-function relationships due to its sensitivity to even small currents and easy manipulation, which allows for screening of thousands of mutated channels (11). We chose to study yeast as a model system due to its powerful genetic tools. Since cellular trafficking is a highly conserved process, we reasoned that secretory pathway conditions that influence a mammalian Kir channel in yeast, would inform us of similar requirements in less genetically amenable mammalian systems. Taking advantage of the yeast deletion library (12) and SGA methodology (13, 14), we found that deletion of *SUR4*, *CSG2*, *ERV14*, *EMP24*, *ERV25*, *BST1*, or *YIL039W*/*TED1* impaired Kir channel functional expression: First, the deletions partially restored yeast growth on high Na^+ media in the presence of the mutated, Na^+ permeable K^+ channel Kir3.2S177W (Kir*). Second, a K^+ selective Kir channel (Kir3.2V188G) was unable to rescue growth on low K^+ media of *trk1*Δ *trk2*Δ yeast also carrying one of the deletions.

A common theme among five of the proteins identified by our screen (Erv14p, Emp24p, Erv25p, Bst1p, and Yil039wp/Ted1p) is that they affect maturation and trafficking of GPI anchored proteins. This was unexpected because Kir channels are transmembrane proteins not known to be modified by a GPI anchor. It is possible that the machinery required for ER exit of GPI anchored proteins has additional functions in trafficking of transmembrane proteins. In fact, deletion of Erv14p leads to ER retention of the transmembrane proteins Axl2p and Sma1p (19, 20). Alternatively, GPI-anchored proteins may indirectly affect Kir channel trafficking. Slowed ER exit of GPI-anchored proteins in *gwt1-10* yeast has been shown to disrupt the formation of lipid domains in the ER and thereby to indirectly affect sorting and budding of transmembrane proteins (36). We speculate that the interplay between different classes of proteins during the formation of lipid microdomains (37) may affect trafficking of Kir channels.

Deletion of the other two candidates identified by our screen, *SUR4* or *CSG2*, alters the lipid composition of yeast cells by reducing synthesis of C_{24} and C_{26} fatty acids (17, 38) or of sphingolipids with mannose modification of their headgroups (39), respectively. The lipid composition of membranes may influence Kir channel functional expression in two ways. First, lipid rafts rich in sphingolipids or their precursor, ceramide, play a role in trafficking at the level of ER exit (40-42) and at the level of protein sorting at the Golgi (43). Second, the local lipid environment at the plasma membrane may influence channel activity. For example, enrichment of membranes with cholesterol induced an inactive channel conformation in Kir2.1 (44) and a specific interaction between the bacterial K^+ channel KcsA and phosphatidylglycerol is required for channel function (45). C_{24} and C_{26} fatty acids are also found in remodeled GPI anchors (46), opening the possibility that deletion of SUR4 affects Kir channel trafficking through indirect effects on GPI-anchored proteins as discussed above.

Our screen identified a phenotype for the previously uncharacterized gene *YIL039W*, which encodes a metallophosphoesterase domain-containing protein conserved in eukaryotes, including humans (MPPE1). Genetic interaction data based on yeast growth (15) and UPR activation, as well as biochemical data showing ER retention of Gas1p in *emp24*Δ, *erv25*Δ (33, 35), and *yil039w*Δ yeast provide evidence that Yil039wp acts together with Emp24p and Erv25p in cargo exit from the ER. We therefore named

YIL039W **T**rafficking of **E**mp24p/Erv25p-dependent cargo **D**isrupted 1 (*TED1*). It is interesting to note that the *bst1*Δ strain, in which Gas1p maturation was also delayed (as previously reported (47)), displayed an aggravating genetic interaction with *ted1*Δ, but buffering interactions with *emp24Δ* and *erv25Δ*. We therefore predict that Bst1p and Ted1p function in parallel pathways to regulate Emp24p/Erv25p function. Since Yil039wp/Ted1p contains a predicted phosphoesterase domain, it will be of interest to identify the targets that are dephosphorylated by Ted1p. One candidate substrate is the amphiphysin homologue Rvs167p, which is phosphorylated by Pho85-Pcl1 (48) and was shown in a large-scale pull down study to physically interact with Ted1p (49)*.

Since Kir3.2 is not native to yeast, our screen was intended to identify global requirements for Kir channel functional expression and probably precluded the identification of specific chaperoning interactions, which would require co-evolution. The seven proteins identified by our screen and their cellular roles are conserved up to mammals, highlighting the appropriate nature of yeast as a model system to uncover basic cellular machinery involved in Kir channel functional expression. The results provide important leads that will allow us to probe deeper into the mechanisms that regulate trafficking and activity of Kir channels in mammalian systems.

Footnote: * Intriguingly, *SUR4* was identified as a suppressor of *rvs161* and *rvs167* (50).

Materials and Methods

Yeast Strains and Media

Yeast strains were picked from the deletion library (12) or constructed by PCR-mediated gene disruption in the BY4742 background (51). Online Table S3 lists strains, primers and plasmids. Yeast media recipes were based on (11, 14) or are provided as Supplemental Methods online.

Yeast Screen

376 yeast strains from the MATa deletion library (online Table S1) (12, 15) were mated to yeast expressing Kir3.2S177W-GFP using SGA methodology (13, 14). The selection scheme is shown online in Table S2. Growth of the double mutant strains was tested on synthetic media containing 750 mM Na^+ and dextrose or galactose. Plates were photographed using a ChemiImager Ready (Alpha Innotech Corp.) and colony sizes, S_{gal} and S_{dex}, measured using software developed by (52). Initial Na^+-tolerant candidates had to meet the criterion that four out of six replicates or the average of the six colony size differences $|S_{gal}*100/S_{dex} - 100|$ were smaller than the average $|S_{gal}*100/S_{dex} - 100|$ for all strains tested minus one standard deviation.

Yeast Assays

Doubling times and growth rates were determined at 30°C by diluting over night cultures to 2 * 10^6 cells/ml and measuring the optical density (OD_{660}) at 0 h and 4 or 8 h later. For growth tests on plates, over night liquid cultures were adjusted to equal ODs and 10-fold serial dilutions plated. Photographs were taken three days after plating. The experiments were repeated at least two times. Yeast protein samples were prepared by the post-alkaline lysis method (53). Western blots were probed with rabbit anti-GIRK2 (Alomone), mouse anti-PGK (Molecular Probes), or rabbit anti-Gas1p (Walter lab) antibodies. Fixed yeast cells were imaged using widefield epifluorescence on a Nikon TE2000 microscope. Images presented are single planes from the middle and top of deconvolved stacks. For the UPR assay, fluorescence signals from 4xUPRE-GFP normalized to TEF2pr-RFP were measured using Flow Cytometry. For detailed procedures see Supplemental Methods.

Statistics

One-way ANOVA followed by Dunnett's test and unpaired t-test were performed with GraphPad Prism 4.0.

Acknowledgements

We thank B. Schwappach for the pYES2 plasmid; C. Boone and A. Tong for yeast strains; J. Haber for the *pma1-105* and control strains; S. Collins for the colony measuring software and help with data analysis; R. Shaw for help with image acquisition and use of the microscope; and members of the Jan and Weissman labs for stimulating discussions. This work is supported by the NIMH MERIT Award R37MH065334. MS is supported by a NIH K99/R00 award, MJ by the National Science Foundation. PW, JW, Y-NJ, and LYJ are HHMI investigators.

Figure Legends

Table 1: Deletions that affect Kir* functional expression.

Figure 1
Deletion of seven early secretory pathway-localized proteins reduced Na^+ toxicity conferred by Kir*. Growth of yeast strains carrying Kir* alone or in combination with the deletions was assayed by 10 fold serial dilutions on agar plates (top) or by doubling time measurements in liquid culture (bottom). (A) Expression of Kir* in control yeast slowed growth in 500 mM Na^+ YPAGR. Growth inhibition by Kir* was partially reversed in yeast strains carrying deletions of seven early secretory pathway-localized proteins. (B) The deletions did not enhance growth in high Na^+ media when Kir* was repressed (500 mM Na^+ YPAD) or (C) in low Na^+ media when Kir* was induced (YPAGR). Whiskers - min. and max., box - 25th to 75th percentile and median, open square - mean, n = 5. # - statistically significant difference compared to yeast expressing Kir* in the control background ($p<0.01$, Dunnett's test).

Figure 2
Hygromycin B sensitivity of deletion strains. Growth rates measured in 500 mM Na^+ YPAGR liquid media with 500 mg/L hygromycin B were normalized to growth rates in 500 mM Na^+ YPAGR. (A) The assay detected hygromycin resistance of *pma1-105* yeast compared to control DBY745 yeast ($p<0.01$, t-test). (B) The seven deletion strains showed no significant difference in hygromycin sensitivity compared to control BY4742 yeast ($p>0.05$, Dunnett's test), although the *csg2*Δ strain showed a tendency toward increased hygromycin sensitivity and the *sur4*Δ and *erv14*Δ strains towards hygromycin resistance. Error bars are standard errors, n=3.

Figure 3
The seven deletions impaired rescue of *trk1*Δ *trk2*Δ yeast by Kir3.2V188G. Ten fold serial dilutions were spotted onto Low Salt plates containing 0.5 mM KCl or 100 mM KCl. (A) *trk1*Δ *trk2*Δ yeast did not grow on 0.5 mM K^+ media. Growth was rescued by expression of Kir3.2V188G. In triple mutant yeast lacking Trk1p, Trk2p, and one of seven early secretory pathway-localized proteins, Kir3.2V188G only partially restored growth on 0.5 mM K^+ media. (B) The triple mutant yeast strains, except *erv14*Δ, grew well on 100 mM K^+ media, where Kir3.2V188G is dispensable for growth.

Figure 4
Total protein levels and distribution of Kir*-GFP. (A) Western blot of yeast expressing Kir* in the control or deletion background was probed with anti-Kir3.2 antibody. A band of similar intensity was detected in all strains carrying Kir*. Phosphoglycerate kinase (PGK) served as a loading control. Molecular weight markers are 100 and 75 for anti-Kir3.2, 50 and 37 kDa for anti-PGK. (B) Deconvolved optical z sections through the middle (left) or periphery (right) of yeast expressing Kir* tagged with eGFP at the C-terminus. In all strains, Kir* localized to the perinuclear and peripheral ER. Scale bar = 2.5 μm.

Figure 5

Ted1p, encoded by *YIL039W*, is involved in trafficking of the GPI-anchored protein Gas1p. (A) *YIL039W*, *EMP24*, and *ERV25* were predicted to act in a concerted manner based on their buffering genetic interactions as determined by (15). (B) UPR induction assayed by expression of GFP from a UPR inducible promoter. Combining deletion of *YIL039W* and *ERV25* did not enhance UPR activation to the extent expected for unrelated genes (e.g. *ALG3*, *OST3*, *SPC2*), suggesting that Yil039wp and Erv25p share a common function. (C) Western blot of whole cell extracts probed with an antibody to Gas1p. Deletion of *YIL039W*/*TED1* led to accumulation of Gas1p in its 100 kDa core glycosylated ER form as previously observed for *emp24*Δ and *erv25*Δ strains (33, 35).

References

1. Neusch, C., Weishaupt, J. H. & Bahr, M. (2003) Cell Tissue Res 311, 131-8.
2. Deutsch, C. (2002) Annu Rev Physiol 64, 19-46.
3. Ruppersberg, J. P. (2000) Pflugers Arch 441, 1-11.
4. Logothetis, D. E., Jin, T., Lupyan, D. & Rosenhouse-Dantsker, A. (2007) Pflugers Arch.
5. Tinker, A. & Jan, L. Y. (1999) Current Topics in Membranes 46, 143-158.
6. Ma, D. & Jan, L. Y. (2002) Curr Opin Neurobiol 12, 287-92.
7. Bichet, D., Haass, F. A. & Jan, L. Y. (2003) Nat Rev Neurosci 4, 957-67.
8. Mark, M. D. & Herlitze, S. (2000) Eur J Biochem 267, 5830-6.
9. Yi, B. A., Lin, Y. F., Jan, Y. N. & Jan, L. Y. (2001) Neuron 29, 657-67.
10. Bichet, D., Lin, Y. F., Ibarra, C. A., Huang, C. S., Yi, B. A., Jan, Y. N. & Jan, L. Y. (2004) Proc Natl Acad Sci U S A 101, 4441-6.
11. Nakamura, R. L. & Gaber, R. F. (1998) Methods Enzymol 293, 89-104.
12. Giaever, G. & others (2002) Nature 418, 387-91.
13. Tong, A. H., Evangelista, M., Parsons, A. B., Xu, H., Bader, G. D., Page, N., Robinson, M., Raghibizadeh, S., Hogue, C. W., Bussey, H., Andrews, B., Tyers, M. & Boone, C. (2001) Science 294, 2364-8.
14. Schuldiner, M., Collins, S. R., Weissman, J. S. & Krogan, N. J. (2006) Methods 40, 344-52.
15. Schuldiner, M., Collins, S. R., Thompson, N. J., Denic, V., Bhamidipati, A., Punna, T., Ihmels, J., Andrews, B., Boone, C., Greenblatt, J. F., Weissman, J. S. & Krogan, N. J. (2005) Cell 123, 507-19.
16. Kubo, Y., Adelman, J. P., Clapham, D. E., Jan, L. Y., Karschin, A., Kurachi, Y., Lazdunski, M., Nichols, C. G., Seino, S. & Vandenberg, C. A. (2005) Pharmacol Rev 57, 509-26.
17. Rossler, H., Rieck, C., Delong, T., Hoja, U. & Schweizer, E. (2003) Mol Genet Genomics 269, 290-8.
18. Uemura, S., Kihara, A., Iwaki, S., Inokuchi, J. & Igarashi, Y. (2007) J Biol Chem 282, 8613-21.
19. Powers, J. & Barlowe, C. (1998) J Cell Biol 142, 1209-22.
20. Nakanishi, H., Suda, Y. & Neiman, A. M. (2007) J Cell Sci 120, 908-16.
21. Kaiser, C. (2000) Proc Natl Acad Sci U S A 97, 3783-5.
22. Tanaka, S., Maeda, Y., Tashima, Y. & Kinoshita, T. (2004) J Biol Chem 279, 14256-63.
23. Fujita, M., Yoko, O. T. & Jigami, Y. (2006) Mol Biol Cell 17, 834-50.
24. Springer, S., Chen, E., Duden, R., Marzioch, M., Rowley, A., Hamamoto, S., Merchant, S. & Schekman, R. (2000) Proc Natl Acad Sci U S A 97, 4034-9.
25. Olkkonen, V. M. & Ikonen, E. (2006) J Cell Sci 119, 5031-45.
26. Rodriguez-Navarro, A. (2000) Biochim Biophys Acta 1469, 1-30.
27. Vallejo, C. G. & Serrano, R. (1989) Yeast 5, 307-19.
28. Perlin, D. S., Brown, C. L. & Haber, J. E. (1988) J Biol Chem 263, 18118-22.
29. Garcia-Arranz, M., Maldonado, A. M., Mazon, M. J. & Portillo, F. (1994) J Biol Chem 269, 18076-82.

30. Ko, C. H., Buckley, A. M. & Gaber, R. F. (1990) Genetics 125, 305-12.
31. Huh, W. K., Falvo, J. V., Gerke, L. C., Carroll, A. S., Howson, R. W., Weissman, J. S. & O'Shea, E. K. (2003) Nature 425, 686-91.
32. Ma, D., Zerangue, N., Raab-Graham, K., Fried, S. R., Jan, Y. N. & Jan, L. Y. (2002) Neuron 33, 715-29.
33. Belden, W. J. & Barlowe, C. (1996) J Biol Chem 271, 26939-46.
34. Marzioch, M., Henthorn, D. C., Herrmann, J. M., Wilson, R., Thomas, D. Y., Bergeron, J. J., Solari, R. C. & Rowley, A. (1999) Mol Biol Cell 10, 1923-38.
35. Elrod-Erickson, M. J. & Kaiser, C. A. (1996) Mol Biol Cell 7, 1043-58.
36. Okamoto, M., Yoko-o, T., Umemura, M., Nakayama, K. & Jigami, Y. (2006) J Biol Chem 281, 4013-23.
37. Hancock, J. F. (2006) Nat Rev Mol Cell Biol 7, 456-62.
38. Oh, C. S., Toke, D. A., Mandala, S. & Martin, C. E. (1997) J Biol Chem 272, 17376-84.
39. Uemura, S., Kihara, A., Inokuchi, J. & Igarashi, Y. (2003) J Biol Chem 278, 45049-55.
40. Toulmay, A. & Schneiter, R. (2007) Biochimie 89, 249-54.
41. Horvath, A., Sutterlin, C., Manning-Krieg, U., Movva, N. R. & Riezman, H. (1994) Embo J 13, 3687-95.
42. Dupre, S. & Haguenauer-Tsapis, R. (2003) Traffic 4, 83-96.
43. Simons, K. & Ikonen, E. (1997) Nature 387, 569-72.
44. Romanenko, V. G., Fang, Y., Byfield, F., Travis, A. J., Vandenberg, C. A., Rothblat, G. H. & Levitan, I. (2004) Biophys J 87, 3850-61.
45. Valiyaveetil, F. I., Zhou, Y. & MacKinnon, R. (2002) Biochemistry 41, 10771-7.
46. Pittet, M. & Conzelmann, A. (2007) Biochim Biophys Acta 1771, 405-20.
47. Vashist, S., Kim, W., Belden, W. J., Spear, E. D., Barlowe, C. & Ng, D. T. (2001) J Cell Biol 155, 355-68.
48. Dephoure, N., Howson, R. W., Blethrow, J. D., Shokat, K. M. & O'Shea, E. K. (2005) Proc Natl Acad Sci U S A 102, 17940-5.
49. Krogan, N. J. & others (2006) Nature 440, 637-43.
50. Desfarges, L., Durrens, P., Juguelin, H., Cassagne, C., Bonneu, M. & Aigle, M. (1993) Yeast 9, 267-77.
51. Brachmann, C. B., Davies, A., Cost, G. J., Caputo, E., Li, J., Hieter, P. & Boeke, J. D. (1998) Yeast 14, 115-32.
52. Collins, S. R., Schuldiner, M., Krogan, N. J. & Weissman, J. S. (2006) Genome Biol 7, R63.
53. Kushnirov, V. V. (2000) Yeast 16, 857-60.

Table 1: Functions of proteins deleted in strains identified by Kir* screen.

name	ORF	localization	function	deletion phenotype
SUR4	YLR372W	ER	Elongase for very long chain fatty acids	Reduced VLCFA levels. Lipid raft association and targeting of H^+ ATPase disrupted. (17, 29, 38, 40)
CSG2	YBR036C	ER	Regulatory subunit of mannosyl-tranferases Csg1p and Csh1p	Reduced mannosylinositol phosphorylceramide levels. (18, 39)
ERV14	YGL054C	ER	COPII vesicle packaging chaperone	ER retention of TM proteins Axl2p and Sma2p. Delay in ER exit of GPI-AP. (19, 20)
EMP24	YGL200C	COPII vesicles	Cargo receptor in p24 protein family	Delay in ER exit of GPI-AP and soluble cargo. Secretion of ER proteins. Suppression of *sec13*Δ. (21, 24, 33-35)
ERV25	YML012W	COPII vesicles	Cargo receptor in p24 protein family	
BST1	YFL025C	ER	GPI inositol deacylase	Delay in ER exit of GPI-AP. Secretion of ER proteins. Suppression *sec13*Δ. (22, 23, 47)
TED1	YIL039W	ER	Uncharacterized	Uncharacterized

Figure 1

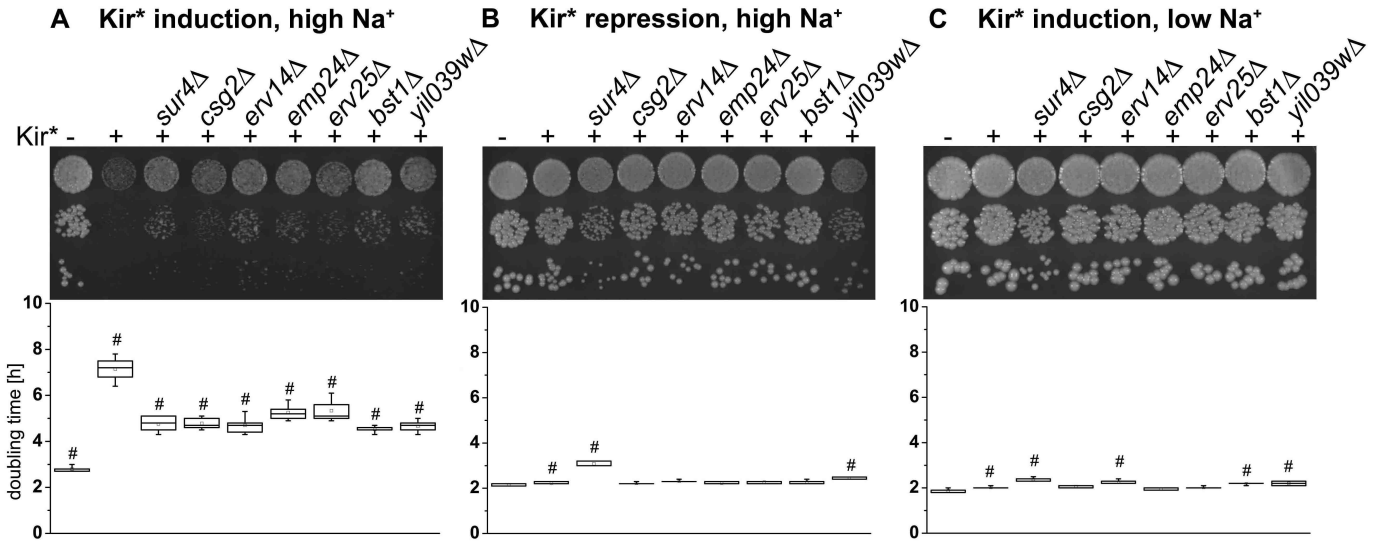
A Kir* induction, high Na+
B Kir* repression, high Na+
C Kir* induction, low Na+
Kir* - + + + + + + + + +
sur4Δ csg2Δ erv14Δ emp24Δ erv25Δ bst1Δ yil039wΔ
doubling time [h]
0 2 4 6 8 10
#

Figure 2

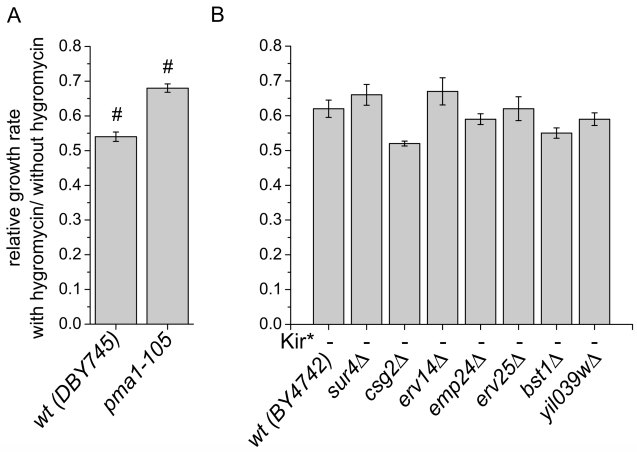
A
B
relative growth rate
with hygromycin/ without hygromycin
0.0
0.1
0.2
0.3
0.4
0.5
0.6
0.7
0.8
#
#
wt (DBY745)
pma1-105
Kir*
wt (BY4742)
sur4Δ
csg2Δ
erv14Δ
emp24Δ
erv25Δ
bst1Δ
yil039wΔ

Figure 3

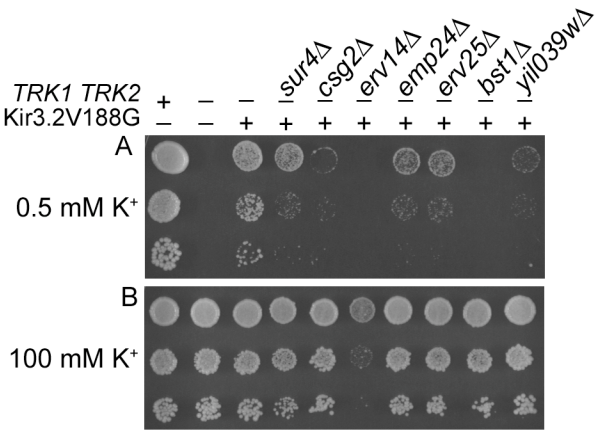
TRK1 TRK2
Kir3.2V188G
sur4Δ
csg2Δ
erv14Δ
emp24Δ
erv25Δ
bst1Δ
yil039wΔ
A
0.5 mM K+
B
100 mM K+

Figure 4

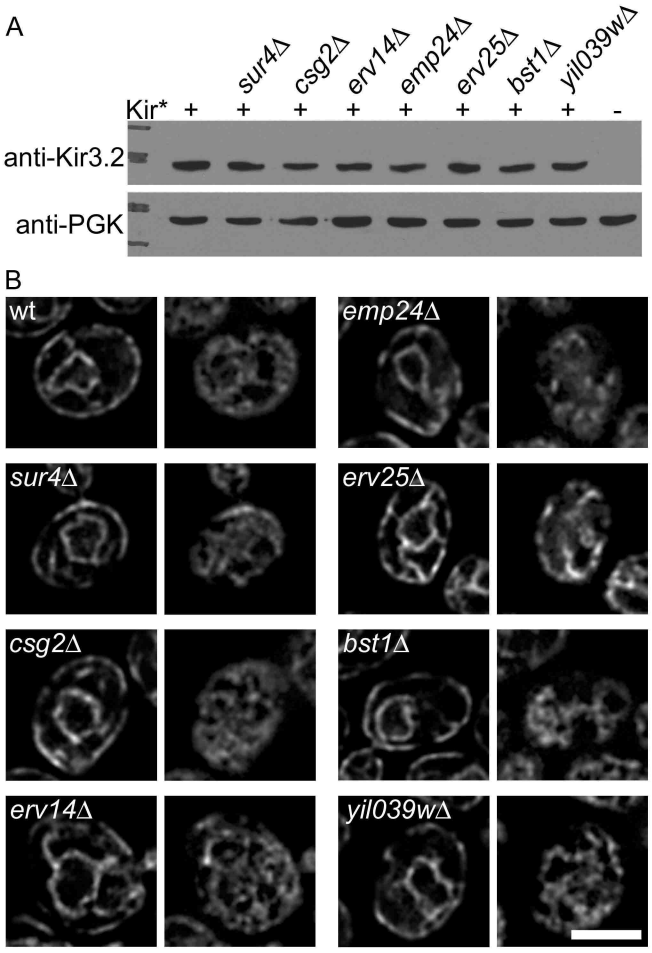
A
sur4Δ
csg2Δ
erv14Δ
emp24Δ
erv25Δ
bst1Δ
yil039wΔ
Kir* + + + + + + + + -
anti-Kir3.2
anti-PGK
B
wt
emp24Δ
sur4Δ
erv25Δ
csg2Δ
bst1Δ
erv14Δ
yil039wΔ

Haass et al. 2007
Figure 5

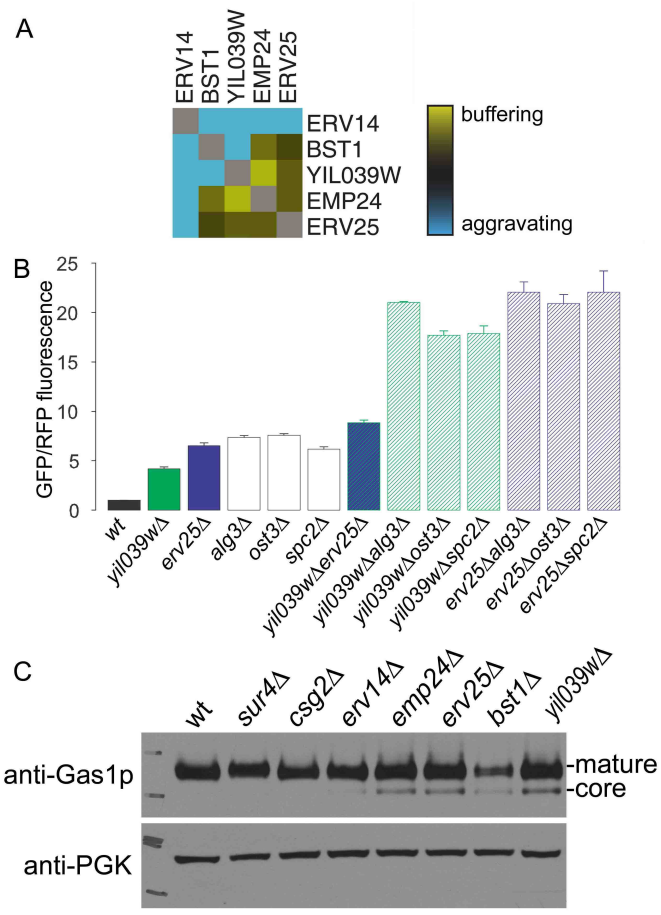

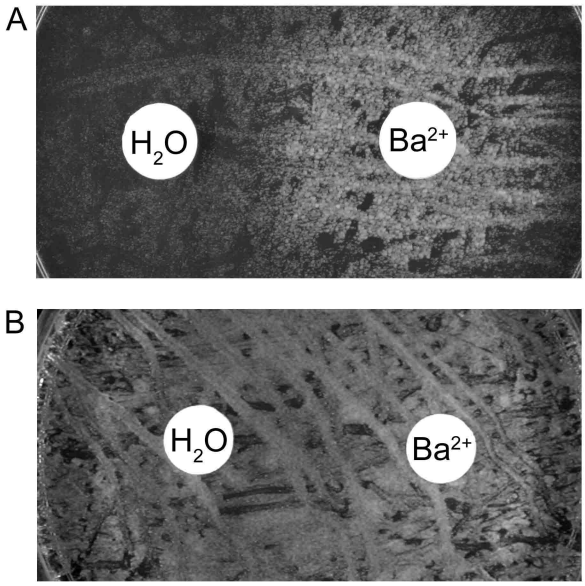

Supplemental Figure S1
Filter disks containing either water or 100 mM BaCl were placed on 500 mM NaCl YPAGR plates with lawns of wildtype yeast carrying (A) or not carrying (B) a genomic insertion of Kir* under a galactose inducible/dextrose repressible promoter. Growth of the Kir* expressing yeast strain was restored in a halo around the disk with barium, but not the disk with water, indicating that growth inhibition was due to Na+ influx through Kir*. Yeast not carrying Kir* grew on the entire plate.

Table S1: yeast deletion strains used in screen

locus	name	function
YCR011C	ADP1	ambiguous
YDR100W	TVP15	ambiguous
YAL026C	DRS2	ambiguous
YDR084C	TVP23	ambiguous
YEL005C	VAB2	ambiguous
YGL084C	GUP1	ambiguous
YDR411C	DFM1	ambiguous
YER004W	FMP52	ambiguous
YGL020C	MDM39	ambiguous
YEL064C	AVT2	ambiguous
YDR233C	RTN1	ambiguous
YDR349C	YPS7	ambiguous
YEL031W	SPF1	ambiguous
YER083C	RMD7	ambiguous
YDR320C	SWA2	ambiguous
YIL090W	ICE2	ambiguous
YIL043C	CBR1	ambiguous
YIL027C	KRE27	ambiguous
YHR039C	MSC7	ambiguous
YHR136C	SPL2	ambiguous
YLR023C	IZH3	ambiguous
YJL178C	ATG27	ambiguous
YKL094W	YJU3	ambiguous
YJL192C	SOP4	ambiguous
YKL179C	COY1	ambiguous
YKL065C	YET1	ambiguous
YLR350W	ORM2	ambiguous
YMR029C	FAR8	ambiguous
YLR250W	SSP120	ambiguous
YNL156C	NSG2	ambiguous
YOR092W	ECM3	ambiguous
YOR198C	BFR1	ambiguous
YOR165W	SEY1	ambiguous
YOR042W	CUE5	ambiguous
YMR251W-A	HOR7	ambiguous
YPR028W	YOP1	ambiguous
YPL246C	RBD2	ambiguous
YPL170W	DAP1	ambiguous
YOR311C	HSD1	ambiguous
YOR307C	SLY41	ambiguous
YOR284W	HUA2	ambiguous
YPR149W	NCE102	ambiguous
YBR162W-A	YSY6	ambiguous
YFR041C	ERJ5	ambiguous
YML048W	GSF2	ambiguous
YDL100C	ARR4	ambiguous
YDR492W	IZH1	ambiguous
YGL161C	YIP5	ambiguous
YNR039C	ZRG17	ambiguous
YCR044C	PER1	ambiguous
YBR177C	EHT1	ambiguous
YBR290W	BSD2	ambiguous
YBR264C	YPT10	ambiguous
YNL008C	ASI3	ambiguous
YML038C	YMD8	ambiguous
YGR089W	NNF2	ambiguous
YJR118C	ILM1	ambiguous
YGR038W	ORM1	ambiguous
YJR134C	SGM1	ambiguous
YER120W	SCS2	ambiguous
YMR052W	FAR3	ambiguous
YBR287W	ZSP1	ambiguous
YMR119W	ASI1	ambiguous
YNL125C	ESBP6	ambiguous
YJL078C	PRY3	ambiguous
YDL072C	YET3	ambiguous
YDR525W	API2	ambiguous
YOL101C	IZH4	ambiguous
YML101C	CUE4	ambiguous
YOL137W	BSC6	ambiguous
YMR065W	KAR5	ambiguous
YHR181W	SVP26	ambiguous
YMR123W	PKR1	ambiguous
YNR075W	COS10	ambiguous
YHR004C	NEM1	ambiguous
YDL222C	FMP45	ambiguous
YJL079C	PRY1	ambiguous
YKR088C	TVP38	ambiguous
YDL204W	RTN2	ambiguous
YDR032C	PST2	ambiguous
YAR044W	OSH1	ambiguous
YEL015W	EDC3	ambiguous
YIL040W	APQ12	ambiguous
YNL065W	MKT1	ambiguous
YER044C	ERG28	ambiguous
YEL003W	GIM4	cytoskeleton assembly
YNL153C	GIM3	cytoskeleton assembly
YMR299C	DYN3	cytoskeleton assembly
YDR424C	DYN2	cytoskeleton assembly
YDR108W	GSG1	ER/Golgi traffic
YAL007C	ERP2	ER/Golgi traffic
YAL042W	ERV46	ER/Golgi traffic
YGL200C	EMP24	ER/Golgi traffic
YGL054C	ERV14	ER/Golgi traffic
YHR110W	ERP5	ER/Golgi traffic
YIL076W	SEC28	ER/Golgi traffic
YIL044C	AGE2	ER/Golgi traffic
YLR080W	EMP46	ER/Golgi traffic
YML012W	ERV25	ER/Golgi traffic
YLR268W	SEC22	ER/Golgi traffic
YOR115C	TRS33	ER/Golgi traffic
YMR292W	GOT1	ER/Golgi traffic
YOR016C	ERP4	ER/Golgi traffic
YCL001W	RER1	ER/Golgi traffic
YDL018C	ERP3	ER/Golgi traffic
YDR524C	AGE1	ER/Golgi traffic
YFL048C	EMP47	ER/Golgi traffic
YNL044W	YIP3	ER/Golgi traffic
YNL049C	SFB2	ER/Golgi traffic
YML067C	ERV41	ER/Golgi traffic
YER122C	GLO3	ER/Golgi traffic
YAR002C-A	ERP1	ER/Golgi traffic
YCR067C	SED4	ER/Golgi traffic
YGR284C	ERV29	ER/Golgi traffic
YNR051C	BRE5	ER/Golgi traffic
YJL117W	PHO86	ER/Golgi traffic
YDL226C	GCS1	ER/Golgi traffic
YGL223C	COG1	ER/Golgi traffic
YBR201W	DER1	ERAD and uibiquitin degradation
YHR204W	MNL1	ERAD and uibiquitin degradation
YMR022W	QRI8	ERAD and uibiquitin degradation
YLR207W	HRD3	ERAD and uibiquitin degradation
YML013W	SEL1	ERAD and uibiquitin degradation
YMR161W	HLJ1	ERAD and uibiquitin degradation
YMR264W	CUE1	ERAD and uibiquitin degradation
YOL013C	HRD1	ERAD and uibiquitin degradation
YDL091C	UBX3	ERAD and uibiquitin degradation
YBR273C	UBX7	ERAD and uibiquitin degradation
YIL030C	SSM4	ERAD and uibiquitin degradation
YDR057W	YOS9	ERAD and uibiquitin degradation
YER151C	UBP3	ERAD and uibiquitin degradation
YOR036W	PEP12	Golgi-endosome-vacuole traffic
YJL029C	VPS53	Golgi-endosome-vacuole traffic
YDR137W	RGP1	Intra Golgi traffic
YGL005C	COG7	Intra Golgi traffic
YHL031C	GOS1	Intra Golgi traffic
YKL212W	SAC1	Intra Golgi traffic
YOR216C	RUD3	Intra Golgi traffic
YOR070C	GYP1	Intra Golgi traffic
YOL018C	TLG2	Intra Golgi traffic
YPL051W	ARL3	Intra Golgi traffic
YBR164C	ARL1	Intra Golgi traffic
YBL102W	SFT2	Intra Golgi traffic
YNL041C	COG6	Intra Golgi traffic
YDL137W	ARF2	Intra Golgi traffic
YJR031C	GEA1	Intra Golgi traffic
YNL051W	COG5	Intra Golgi traffic
YML071C	COG8	Intra Golgi traffic
YLR039C	RIC1	Intra Golgi traffic
YDL192W	ARF1	Intra Golgi traffic
YEL022W	GEA2	Intra Golgi traffic
YBL011W	SCT1	Lipid biosynthesis
YBR183W	YPC1	Lipid biosynthesis
YDR294C	DPL1	Lipid biosynthesis
YDR297W	SUR2	Lipid biosynthesis
YGR202C	PCT1	Lipid biosynthesis
YGR170W	PSD2	Lipid biosynthesis
YGR157W	CHO2	Lipid biosynthesis
YHL003C	LAG1	Lipid biosynthesis
YKL020C	SPT23	Lipid biosynthesis
YKL140W	TGL1	Lipid biosynthesis
YKL008C	LAC1	Lipid biosynthesis
YJL134W	LCB3	Lipid biosynthesis
YLL043W	FPS1	Lipid biosynthesis
YJL196C	ELO1	Lipid biosynthesis
YLR372W	SUR4	Lipid biosynthesis
YOR245C	DGA1	Lipid biosynthesis
YNL323W	LEM3	Lipid biosynthesis
YOR049C	RSB1	Lipid biosynthesis
YOR171C	LCB4	Lipid biosynthesis
YMR272C	SCS7	Lipid biosynthesis
YOR377W	ATF1	Lipid biosynthesis
YOL065C	INP54	Lipid biosynthesis
YPL087W	YDC1	Lipid biosynthesis
YDL052C	SLC1	Lipid biosynthesis
YJR073C	OPI3	Lipid biosynthesis
YDR503C	LPP1	Lipid biosynthesis
YML059C	NTE1	Lipid biosynthesis
YGL126W	SCS3	Lipid biosynthesis
YIL124W	AYR1	Lipid biosynthesis
YKR067W	GPT2	Lipid biosynthesis
YIR033W	MGA2	Lipid biosynthesis
YNL130C	CPT1	Lipid biosynthesis
YKR053C	YSR3	Lipid biosynthesis
YCR034W	FEN1	Lipid biosynthesis
YBR159W	YBR159W	Lipid biosynthesis
YHR123W	EPT1	Lipid biosynthesis
YOR317W	FAA1	Lipid biosynthesis
YMR313C	TGL3	Lipid biosynthesis
YBR036C	CSG2	Lipid biosynthesis
YPR135W	CTF4	miscellaneous, chromatin adhesion
YJL168C	SET2	miscellaneous, histone methyltransferase
YHR135C	YCK1	miscellaneous, kinase
YBL082C	RHK1	N-linked glycosylation
YAL058W	CNE1	N-linked glycosylation
YGR036C	CAX4	N-linked glycosylation
YGL226C-A	OST5	N-linked glycosylation
YML019W	OST6	N-linked glycosylation
YOR002W	ALG6	N-linked glycosylation
YOR067C	ALG8	N-linked glycosylation
YNL219C	ALG9	N-linked glycosylation
YPL227C	ALG5	N-linked glycosylation
YGR227W	DIE2	N-linked glycosylation
YNR030W	ECM39	N-linked glycosylation
YJR131W	MNS1	N-linked glycosylation
YOR085W	OST3	N-linked glycosylation
YDL232W	OST4	N-linked glycosylation
YCR017C	CWH43	O-linked glycosylation, GPI, cell wall biosynthesis
YEL004W	YEA4	O-linked glycosylation, GPI, cell wall biosynthesis
YMR215W	GAS3	O-linked glycosylation, GPI, cell wall biosynthesis
YLR120C	YPS1	O-linked glycosylation, GPI, cell wall biosynthesis
YNL327W	EGT2	O-linked glycosylation, GPI, cell wall biosynthesis
YMR307W	GAS1	O-linked glycosylation, GPI, cell wall biosynthesis
YOL030W	GAS5	O-linked glycosylation, GPI, cell wall biosynthesis
YBR067C	TIP1	O-linked glycosylation, GPI, cell wall biosynthesis
YLR390W-A	CCW14	O-linked glycosylation, GPI, cell wall biosynthesis
YER005W	YND1	O-linked glycosylation, GPI, Golgi glycosylation
YEL042W	GDA1	O-linked glycosylation, GPI, Golgi glycosylation
YDR483W	KRE2	O-linked glycosylation, GPI, Golgi glycosylation
YBR229C	ROT2	O-linked glycosylation, GPI, GPI anchor biosynthesis
YFL025C	BST1	O-linked glycosylation, GPI, GPI anchor biosynthesis
YJL062W	LAS21	O-linked glycosylation, GPI, GPI anchor biosynthesis
YAL023C	PMT2	O-linked glycosylation, GPI, O-linked glycosylation
YGL027C	CWH41	O-linked glycosylation, GPI, O-linked glycosylation
YGR199W	PMT6	O-linked glycosylation, GPI, O-linked glycosylation
YHR142W	CHS7	O-linked glycosylation, GPI, O-linked glycosylation
YOR321W	PMT3	O-linked glycosylation, GPI, O-linked glycosylation
YDL093W	PMT5	O-linked glycosylation, GPI, O-linked glycosylation
YDL095W	PMT1	O-linked glycosylation, GPI, O-linked glycosylation
YBL017C	PEP1	Post-Golgi traffic
YEL013W	VAC8	Post-Golgi traffic
YMR183C	SSO2	Post-Golgi traffic
YNL297C	MON2	Post-Golgi traffic
YOR089C	VPS21	Post-Golgi traffic
YPL195W	APL5	Post-Golgi traffic
YPR173C	VPS4	Post-Golgi traffic
YDR484W	VPS52	Post-Golgi traffic
YGR261C	APL6	Post-Golgi traffic
YJL024C	APS3	Post-Golgi traffic
YJL004C	SYS1	Post-Golgi traffic
YBR288C	APM3	Post-Golgi traffic
YDL231C	BRE4	Post-Golgi traffic
YIL005W	EPS1	Protein maturation, disulfide bond formation
YHR176W	FMO1	Protein maturation, disulfide bond formation
YOR288C	MPD1	Protein maturation, disulfide bond formation
YDR518W	EUG1	Protein maturation, disulfide bond formation
YIR038C	GTT1	Protein maturation, disulfide bond formation
YOL088C	MPD2	Protein maturation, disulfide bond formation
YGL203C	KEX1	Protein maturation, protein maturation
YDR304C	CPR5	Protein maturation, protein maturation
YDR410C	STE14	Protein maturation, protein maturation
YMR214W	SCJ1	Protein maturation, protein maturation
YMR152W	YIM1	Protein maturation, protein maturation
YNL238W	KEX2	Protein maturation, protein maturation
YMR274C	RCE1	Protein maturation, protein maturation
YDR519W	FPR2	Protein maturation, protein maturation
YLR246W	ERF2	Protein maturation, protein maturation
YOL110W	SHR5	Protein maturation, protein maturation
YJL073W	JEM1	Protein maturation, protein maturation
YJR117W	STE24	Protein maturation, protein maturation
YKL119C	VPH2	Protein maturation, vATPase complex assembly
YHR060W	VMA22	Protein maturation, vATPase complex assembly
YGR105W	VMA21	Protein maturation, vATPase complex assembly
YGL012W	ERG4	Steroid/sterol biosynthesis
YGR177C	ATF2	Steroid/sterol biosynthesis
YLR056W	ERG3	Steroid/sterol biosynthesis
YMR015C	ERG5	Steroid/sterol biosynthesis
YML008C	ERG6	Steroid/sterol biosynthesis
YMR202W	ERG2	Steroid/sterol biosynthesis
YLR242C	ARV1	Steroid/sterol biosynthesis
YNL280C	ERG24	Steroid/sterol biosynthesis
YDL019C	OSH2	Steroid/sterol biosynthesis
YNR019W	ARE2	Steroid/sterol biosynthesis
YNR008W	LRO1	Steroid/sterol biosynthesis
YML075C	HMG1	Steroid/sterol biosynthesis
YCR048W	ARE1	Steroid/sterol biosynthesis
YLR450W	HMG2	Steroid/sterol biosynthesis
YGR086C	PIL1	TOR/PKC signalling
YJR066W	TOR1	TOR/PKC signalling
YIL105C	SLM1	TOR/PKC signalling
YER019C-A	SBH2	translocation
YKL073W	LHS1	translocation
YLR292C	SEC72	translocation
YOL031C	SIL1	translocation
YBR171W	SEC66	translocation
YML055W	SPC2	translocation
YBR283C	SSH1	translocation
YJR010C-A	SPC1	translocation
YER087C-B	SBH1	translocation
YLL052C	AQY2	transport
YLL028W	TPO1	transport
YMR054W	STV1	transport
YCL025C	AGP1	transport, amino acid transport
YLR220W	CCC1	transport, Ca transport
YGL167C	PMR1	transport, Ca transport
YDR270W	CCC2	transport, heavy metal transport
YOR079C	ATX2	transport, heavy metal transport
YDR205W	MSC2	transport, heavy metal transport
YJR040W	GEF1	transport, heavy metal transport
YLR130C	ZRT2	transport, heavy metal transport
YBR132C	AGP2	transport, not in Maya's paper
YJL198W	PHO90	transport, phosphate transport
YBR106W	PHO88	transport, phosphate transport
YNR013C	PHO91	transport, phosphate transport
YJL212C	OPT1	transport, sulfur transport
YPL274W	SAM3	transport, sulfur transport
YHR079C	IRE1	unfolded protein response
YDR056C	YDR056C	unknown
YCL056C	YCL056C	unknown
YCL045C	YCL045C	unknown
YEL001C	YEL001C	unknown
YDR307W	YDR307W	unknown
YEL043W	YEL043W	unknown
YGL010W	YGL010W	unknown
YDR221W	YDR221W	unknown
YDR222W	YDR222W	unknown
YDR357C	YDR357C	unknown
YDR344C	YDR344C	unknown
YER071C	YER071C	unknown
YIL039W	YIL039W	unknown
YGL231C	YGL231C	unknown
YLL014W	YLL014W	unknown
YLR064W	YLR064W	unknown
YLR042C	YLR042C	unknown
YJL171C	YJL171C	unknown
YLL055W	YLL055W	unknown
YKL063C	YKL063C	unknown
YLL023C	YLL023C	unknown
YMR010W	YMR010W	unknown
YLR194C	YLR194C	unknown
YMR163C	YMR163C	unknown
YMR031C	YMR031C	unknown
YOR214C	YOR214C	unknown
YNL194C	YNL194C	unknown
YNL190W	YNL190W	unknown
YOR175C	YOR175C	unknown
YOR044W	YOR044W	unknown
YMR253C	YMR253C	unknown
YPR003C	YPR003C	unknown
YOL047C	YOL047C	unknown
YPL207W	YPL207W	unknown
YPL206C	YPL206C	unknown
YOR285W	YOR285W	unknown
YOR291W	YOR291W	unknown
YPR148C	YPR148C	unknown
YBR052C	YBR052C	unknown
YPR114W	YPR114W	unknown
YPR063C	YPR063C	unknown
YPR071W	YPR071W	unknown
YDL121C	YDL121C	unknown
YJR088C	YJR088C	unknown
YDL099W	YDL099W	unknown
YGR263C	YGR263C	unknown
YGR266W	YGR266W	unknown
YNL146W	YNL146W	unknown
YCR043C	YCR043C	unknown
YNR021W	YNR021W	unknown
YCR061W	YCR061W	unknown
YNL046W	YNL046W	unknown
YGR106C	YGR106C	unknown
YER113C	YER113C	unknown
YJR015W	YJR015W	unknown
YNL095C	YNL095C	unknown
YPL137C	YPL137C	unknown
YGR130C	YGR130C	unknown
YBR255W	YBR255W	unknown
YDR476C	YDR476C	unknown
YOL107W	YOL107W	unknown
YHR045W	YHR045W	unknown
YLR050C	YLR050C	unknown
YJL123C	YJL123C	unknown
YBR096W	YBR096W	unknown
YER053C-A	YER053C-A	unknown
YNL300W	TOS6	unknown
YIL016W	SNL1	unknown
YML128C	MSC1	unknown
undefin	NO GENE	

ambiguous	85
unknown	69
lipid biosynthesis	53
ER/Golgi traffic	29
O-linked glycosylation, GPI	22
protein maturation	21
intra-Golgi traffic	18
transport	17
N-linked glycosylation	14
ERAD and ubiquitin degradation	13
post-Golgi traffic	13
translocation	9
cytoskelton assembly	4
TOR/PKC signaling	3
miscellaneous	3
Golgi-endosome-vacuole traffic	2
UPR	1
	376

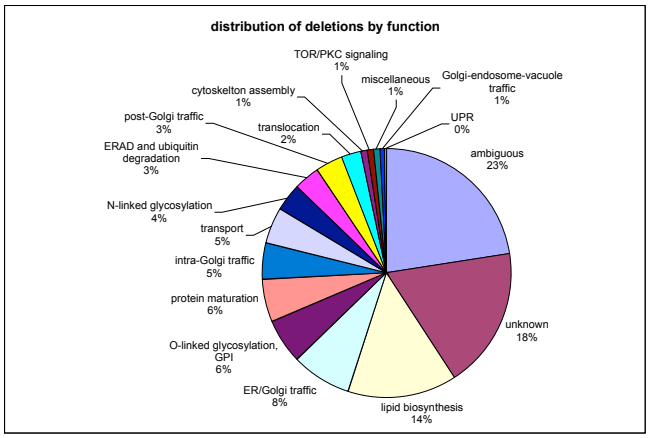

Table S2: Yeast screen selection scheme

MATalpha: ura3Δ::URA3/GAL1pr-Kir3.2S177W-GFP can1Δ::STE2pr-spHIS5 lyp1Δ::STE3pr-LEU2 LYS2+ his3Δ1 leu2Δ0 cyh2

MATa: YYYΔ::Kan^r CAN1 LYP1 LYS2+ his3Δ1 leu2Δ0 ura3Δ0 met15Δ0

Step	Media	Time	Temp.	Gentotype
1.a MATalpha 1.b MATa	SD(MSG)-URA YPAD+G418	2 days	30ºC	
2. Mating	YPAD	1 day	RT	
3. Diploid selection	SD(MSG)-URA+G418	2 days	30ºC	
4. Sporulation	sporulation media	5 days	22ºC	
5. Haploid selection 1	SD(MSG) –HIS–ARG–LYS +CAN +S-AEC	2 days	30ºC	can1Δ::STE2pr-HIS3, lyp1Δ
6. Haploid selection 2	SD(MSG) –HIS–ARG–LYS +CAN +S-AEC	1 day	30ºC	can1Δ::STE2pr-HIS3, lyp1Δ
7. Double mutant selection 1	SD(MSG) –HIS–ARG–LYS–URA +CAN +S-AEC +G418	2 days	30ºC	can1Δ::STE2pr-HIS3, lyp1Δ, YYYΔ::Kan^r, ura3Δ::URA3/ GAL1pr-S177W-GFP
8. Double mutant selection 2	SD(MSG) –HIS–ARG–LYS–URA +CAN +S-AEC +G418	2 days	30ºC	can1Δ::STE2pr-HIS3, lyp1Δ, YYYΔ::Kan^r, ura3Δ::URA3/ GAL1pr-S177W-GFP
9. Tests	750 Na SD(MSG) –HIS–ARG–LYS–URA +CAN +S-AEC +G418 750 Na SGR(MSG) –HIS–ARG–LYS–URA +CAN +S-AEC +G418	2 days	30ºC	can1Δ::STE2pr-HIS3, lyp1Δ, YYYΔ::Kan^r, ura3Δ::URA3/ GAL1pr-S177W-GFP

Table S3: Yeast strains used in this study and primers used to generate these strains

name	genotype	plasmid	forward primer for genome insertion	reverse primer for genome insertion	forward primer for check PCR	reverse primer for check PCR
YMS613	MATalpha can1Δ::STE2pr-spHIS5 lyp1Δ::STE3pr-LEU2 LYS2+ his3Δ1 leu2Δ0 ura3Δ cyh2 #					
YMS614	YMS613 + sur4Δ::Kan^r	pFA6a KAN MX6	ATTCGGCTTTTTTCCGTTTGTTTACGAAACATA AACAGTCGGTCGACGGATCCCCGGGTT	TTTTCTTTTTCATTCGCTGTCAAAAATTCTCGCT TCCTATTCGATGAATTCGAGCTCGTT	TGGTTTTTGACAGCT CTTCACTCG	GTATTCTGGGCCTC CATGTCG
YMS615	YMS613 + csg2Δ::Kan^r	pFA6a KAN MX6	GCTGGTGAGTTAGCACGATAACAAACAAAGAT ACAGCGTCGGTCGACGGATCCCCGGGTT	TGTTACATCATCATCAGTCATATAAAGTATGTT GTCCGTATCGATGAATTCGAGCTCGTT	GAGGCATGGTACTC CTTCTTATTC	GTATTCTGGGCCTC CATGTCG
YMS616	YMS613 + erv14Δ::Kan^r	pFA6a KAN MX6	CAATTAAAGTAAAGTAAAAAAATTAAGAATAAAA AGAAAAGGTCGACGGATCCCCGGGTT	TGGCCCTTCAGTCTTCTTTGGATTTCAATGTCT TGTTGGATCGATGAATTCGAGCTCGTT	TTAATACGAAGGAG AGACCTGG	GTATTCTGGGCCTC CATGTCG
YMS617	YMS613 + emp24Δ::Kan^r	pFA6a KAN MX6	TTAATAGTATCCCTCCGCACAAAAATACACACG CATAAGGGGTCGACGGATCCCCGGGTT	GCAAAAGTAAATAGATATGAACTACATTTTCCT GCTTTACTCGATGAATTCGAGCTCGTT	GACGCGAGGAAAGT CAGAAAAG	GTATTCTGGGCCTC CATGTCG
YMS618	YMS613 + erv25Δ::Kan^r	pFA6a KAN MX6	TATAACTCAGTTGATCTCATAAGTGAAAAGCAA AAAAAGGGGTCGACGGATCCCCGGGTT	AGCTGATACACAAATGCATGGTGTGGTCCTCT TCCTTTGCTCGATGAATTCGAGCTCGTT	CGCGTACAAAGAGT TTCTGG	GTATTCTGGGCCTC CATGTCG
YMS619	YMS613 + bst1Δ::Kan^r	pFA6a KAN MX6	TATCTTAGGCTTACCATCATACAAAAATCTTCAT TTCGTTGGTCGACGGATCCCCGGGTT	GCAATATATACAGTTAATCTTTTTTTACTGGGTT GTAGTTTCGATGAATTCGAGCTCGTT	GGCGCGAATTTTGA AAAAGG	GTATTCTGGGCCTC CATGTCG
YMS620	YMS613 + YIL039WΔ::Kan^r	pFA6a KAN MX6	CTGAAAACAACAGCAGCAGCATTGTACCAAGA ATCCCAAGGGTCGACGGATCCCCGGGTT	ATCTCTATACAGGAGTTTTATCTTCTTTACTCTT TTTTGTTCGATGAATTCGAGCTCGTT	GCTAGATTCCTCCC CTAGTCAC	GTATTCTGGGCCTC CATGTCG
YMS621	MATalpha can1Δ::STE2pr-spHIS5 lyp1Δ::STE3pr-LEU2 LYS2+ his3Δ1 leu2Δ0 ura3Δ::URA3/GAL1pr-no insert cyh2	empty pYES2-2micron origin ###	AGTTTTGACCATCAAAGAAGGTTAATGTGGCTG TGGTTTCgggtaataactgatataatt	AGCTTTTTCTTTCCAATTTTTTTTTTTTTCGTCATT ATAGAgcaaattaaagccttcgagc	CGACGTTGAAATTG AGGCTACTGCGCCA	GCGGCCAGCAAAAC TAAAAAACTGTATT
YMS622	MATalpha can1Δ::STE2pr-spHIS5 lyp1Δ::STE3pr-LEU2 LYS2+ his3Δ1 leu2Δ0 ura3Δ::URA3/GAL1pr-Kir3.2S177W-GFP cyh2	Kir3.2S177W-GFP in pYES2-2micron origin ##	AGTTTTGACCATCAAAGAAGGTTAATGTGGCTG TGGTTTCgggtaataactgatataatt	AGCTTTTTCTTTCCAATTTTTTTTTTTTTCGTCATT ATAGAgcaaattaaagccttcgagc	CGACGTTGAAATTG AGGCTACTGCGCCA	GCGGCCAGCAAAAC TAAAAAACTGTATT
YMS623	YMS622 + sur4Δ::Kan^r	pFA6a KAN MX6	ATTCGGCTTTTTTCCGTTTGTTTACGAAACATA AACAGTCGGTCGACGGATCCCCGGGTT	TTTTCTTTTTCATTCGCTGTCAAAAATTCTCGCT TCCTATTCGATGAATTCGAGCTCGTT	TGGTTTTTGACAGCT CTTCACTCG	GTATTCTGGGCCTC CATGTCG
YMS624	YMS622 + csg2Δ::Kan^r	pFA6a KAN MX6	GCTGGTGAGTTAGCACGATAACAAACAAAGAT ACAGCGTCGGTCGACGGATCCCCGGGTT	TGTTACATCATCATCAGTCATATAAAGTATGTT GTCCGTATCGATGAATTCGAGCTCGTT	GAGGCATGGTACTC CTTCTTATTC	GTATTCTGGGCCTC CATGTCG
YMS625	YMS622 + erv14Δ::Kan^r	pFA6a KAN MX6	CAATTAAAGTAAAGTAAAAAAATTAAGAATAAAA AGAAAAGGTCGACGGATCCCCGGGTT	TGGCCCTTCAGTCTTCTTTGGATTTCAATGTCT TGTTGGATCGATGAATTCGAGCTCGTT	TTAATACGAAGGAG AGACCTGG	GTATTCTGGGCCTC CATGTCG
YMS626	YMS622 + emp24Δ::Kan^r	pFA6a KAN MX6	TTAATAGTATCCCTCCGCACAAAAATACACACG CATAAGGGGTCGACGGATCCCCGGGTT	GCAAAAGTAAATAGATATGAACTACATTTTCCT GCTTTACTCGATGAATTCGAGCTCGTT	GACGCGAGGAAAGT CAGAAAAG	GTATTCTGGGCCTC CATGTCG
YMS627	YMS622 + erv25Δ::Kan^r	pFA6a KAN MX6	TATAACTCAGTTGATCTCATAAGTGAAAAGCAA AAAAAGGGGTCGACGGATCCCCGGGTT	AGCTGATACACAAATGCATGGTGTGGTCCTCT TCCTTTGCTCGATGAATTCGAGCTCGTT	CGCGTACAAAGAGT TTCTGG	GTATTCTGGGCCTC CATGTCG
YMS628	YMS622 + bst1Δ::Kan^r	pFA6a KAN MX6	TATCTTAGGCTTACCATCATACAAAAATCTTCAT TTCGTTGGTCGACGGATCCCCGGGTT	GCAATATATACAGTTAATCTTTTTTTACTGGGTT GTAGTTTCGATGAATTCGAGCTCGTT	GGCGCGAATTTTGA AAAAGG	GTATTCTGGGCCTC CATGTCG
YMS629	YMS622 + YIL039WΔ::Kan^r	pFA6a KAN MX6	CTGAAAACAACAGCAGCAGCATTGTACCAAGA ATCCCAAGGGTCGACGGATCCCCGGGTT	ATCTCTATACAGGAGTTTTATCTTCTTTACTCTT TTTTGTTCGATGAATTCGAGCTCGTT	GCTAGATTCCTCCC CTAGTCAC	GTATTCTGGGCCTC CATGTCG
YMS630	MATalpha trk1Δ::URA3/MET25pr-empty trk2Δ::Nat^r can1Δ::STE2pr-spHIS5 lyp1Δ::STE3pr-LEU2 LYS2+ his3Δ1 leu2Δ0 ura3Δ0 cyh2	empty pYESMET25-2micron origin ### and pFA6a NAT	trk1Δ:CATTTTACTTAAAGTTATTACCTTTTTTTGA TAACTAACAgggtaataactgatataatt trk2Δ:TGTACTATTCACCGACGATAAGAGGCTGT AAGAACCACTCGGTCGACGGATCCCCGGGTT	trk1Δ:TTGAGTACGAAAACCTATTTCTAAAGAAT GAGTATATATGgcaaattaaagccttcgagc trk2Δ:ACGTTGGCTCTTATGTAGGTAAAGAGGG GTAAACTTGATTTCGATGAATTCGAGCTCGTT	trk1Δ:CCTTTCGCCCA TTGTTTTTA trk2Δ:GTTTCCCGTTT CTCTCTTTCAC	trk1Δ:GCGGGCCAGCA AAACTAAAAAACTGT ATT trk2Δ:GTATTCTGGGC CTCCATGTCG
YMS631	MATalpha trk1Δ::URA3/MET25pr-Kir3.2V188G-GFP trk2Δ::Nat^r can1Δ::STE2pr-spHIS5 lyp1Δ::STE3pr-LEU2 LYS2+ his3Δ1 leu2Δ0 ura3Δ0 cyh2	Kir3.2V188G-GFP in pYESMET25-2micron origin ## and pFA6a NAT	trk1Δ:CATTTTACTTAAAGTTATTACCTTTTTTTGA TAACTAACAgggtaataactgatataatt trk2Δ:TGTACTATTCACCGACGATAAGAGGCTGT AAGAACCACTCGGTCGACGGATCCCCGGGTT	trk1Δ:TTGAGTACGAAAACCTATTTCTAAAGAAT GAGTATATATGgcaaattaaagccttcgagc trk2Δ:ACGTTGGCTCTTATGTAGGTAAAGAGGG GTAAACTTGATTTCGATGAATTCGAGCTCGTT	trk1Δ:CCTTTCGCCCA TTGTTTTTA trk2Δ:GTTTCCCGTTT CTCTCTTTCAC	trk1Δ:GCGGGCCAGCA AAACTAAAAAACTGT ATT trk2Δ:GTATTCTGGGC CTCCATGTCG
YMS632	YMS631 + sur4Δ::Kan^r	pFA6a KAN MX6	ATTCGGCTTTTTTCCGTTTGTTTACGAAACATA AACAGTCGGTCGACGGATCCCCGGGTT	TTTTCTTTTTCATTCGCTGTCAAAAATTCTCGCT TCCTATTCGATGAATTCGAGCTCGTT	TGGTTTTTGACAGCT CTTCACTCG	GTATTCTGGGCCTC CATGTCG
YMS633	YMS631 + csg2Δ::Kan^r	pFA6a KAN MX6	GCTGGTGAGTTAGCACGATAACAAACAAAGAT ACAGCGTCGGTCGACGGATCCCCGGGTT	TGTTACATCATCATCAGTCATATAAAGTATGTT GTCCGTATCGATGAATTCGAGCTCGTT	GAGGCATGGTACTC CTTCTTATTC	GTATTCTGGGCCTC CATGTCG
YMS634	YMS631 + erv14Δ::Kan^r	pFA6a KAN MX6	CAATTAAAGTAAAGTAAAAAAATTAAGAATAAAA AGAAAAGGTCGACGGATCCCCGGGTT	TGGCCCTTCAGTCTTCTTTGGATTTCAATGTCT TGTTGGATCGATGAATTCGAGCTCGTT	TTAATACGAAGGAG AGACCTGG	GTATTCTGGGCCTC CATGTCG
YMS635	YMS631 + emp34Δ::Kan^r	pFA6a KAN MX6	TTAATAGTATCCCTCCGCACAAAAATACACACG CATAAGGGGTCGACGGATCCCCGGGTT	GCAAAAGTAAATAGATATGAACTACATTTTCCT GCTTTACTCGATGAATTCGAGCTCGTT	GACGCGAGGAAAGT CAGAAAAG	GTATTCTGGGCCTC CATGTCG
YMS636	YMS631 + erv25Δ::Kan^r	pFA6a KAN MX6	TATAACTCAGTTGATCTCATAAGTGAAAAGCAA AAAAAGGGGTCGACGGATCCCCGGGTT	AGCTGATACACAAATGCATGGTGTGGTCCTCT TCCTTTGCTCGATGAATTCGAGCTCGTT	CGCGTACAAAGAGT TTCTGG	GTATTCTGGGCCTC CATGTCG
YMS637	YMS631 + bst1Δ::Kan^r	pFA6a KAN MX6	TATCTTAGGCTTACCATCATACAAAAATCTTCAT TTCGTTGGTCGACGGATCCCCGGGTT	GCAATATATACAGTTAATCTTTTTTTACTGGGTT GTAGTTTCGATGAATTCGAGCTCGTT	GGCGCGAATTTTGA AAAAGG	GTATTCTGGGCCTC CATGTCG
YMS638	YMS631 + YIL039WΔ::Kan^r	pFA6a KAN MX6	CTGAAAACAACAGCAGCAGCATTGTACCAAGA ATCCCAAGGGTCGACGGATCCCCGGGTT	ATCTCTATACAGGAGTTTTATCTTCTTTACTCTT TTTTGTTCGATGAATTCGAGCTCGTT	GCTAGATTCCTCCC CTAGTCAC	GTATTCTGGGCCTC CATGTCG
deletion library	MATa: YYYΔ::Kan^r CAN1 LYP1 LYS2+ his3Δ1 leu2Δ0 ura3Δ0 met15Δ0	pFA6a KAN MX6	see Saccharomyces Genome Deletion Project (http://www-sequence.stanford.edu/group/yeast_deletion_project/deletions3.html)			
YMS660	MATalpha *ade1-100 leu2-3 leu2-112 ura3-52* ####					
YMS661	MATalpha *ade1-100 leu2-3 leu2-112 ura3-52 MAL2* transformed with *pma1-105 ::URA3* fragment ####					

strain BY4742 provided by Charles Boone and Amy Tong, reference: Tong et al. 2001, Science Vol. 294 pp2364-2368

Mouse Kir3.2S177W and Kir3.2V188G (Yi et al, 2001, Neuron, Vol. 29, pp. 657-667; Bichet et al. 2004, PNAS Vol. 101, No. 13, pp. 4441-4446) were cloned into pYES2 (Invitrogen) and pYESMET25 (Minor et al. 1999, Cell, Vol. 96, pp. 879-891), respectively. The 2μ origin was removed using NdeI and NgoMIV followed by blunt end ligation. Channels were tagged with eGFP (Clontech) at the C-terminus.

pYES2-2μ origin and pYESMET25-2μ origin without inserts were used as PCR templates.

kind gift of James E. Haber, strain YMS660 = A612 in Haber lab collection, YMS661 = SN19, reference: Perlin et al. 1988, JBC Vol. 263, No. 34, pp. 18118-18122

Supplemental methods

Yeast Strains

Yeast strains were either picked from the yeast deletion library (1) or re-constructed by PCR-mediated gene disruption in a BY4742 (2) derived background (MATalpha *can1*Δ::STE2pr-*spHIS5 lyp1*Δ::STE3pr-*LEU2 LYS2*$^+$ *MET*$^+$ *his3*Δ1 *leu2*Δ0 *ura3*Δ *cyh2*, a kind gift from Amy Tong and Charles Boone). Online Table S3 lists strains, primers and plasmids. Mouse Kir3.2S177W and Kir3.2V188G (3, 4) were cloned into pYES2 (Invitrogen) and pYESMET25 (5), respectively. Channels were tagged with eGFP (Clontech) at the C-terminus. For integration into the yeast genome, the 2μ origin was removed from pYES2 and pYESMET25 using NdeI and NgoMIV followed by blunt end ligation. Integration of gene disruption cassettes was confirmed by colony PCR.

Yeast Media

Synthetic media (SD or SGR) was prepared from 1.7 g yeast nitrogen base without amino acid and without ammonium sulfate (Difco), 2 g amino acid drop out powder containing all amino acids except those used for selection (6) (amino acids from Sigma), 1 g monosodium glutamic acid (Sigma), and either 20 g dextrose (Riedel-de Haen) or 20 g galactose (Sigma) and 20 g raffinose (Acros) in 1 liter water. Rich media (YPAD or YPAGR) was prepared from 10 g yeast extract (Difco), 20 g peptone (Difco), 120 mg adenine (Sigma) and either 20 g dextrose or 20 g galactose and 20 g raffinose in 1 liter water. Yeast plates contained 2% agar (Difco). For high sodium tests, 500 mM NaCl (Fisher) was added to the media. Geneticin (Invitrogen) was used at 200 mg/l, ClonNat (Werner Biotechnology) at 100 mg/l, hygromycin (Invitrogen) at 500 mg/l. Low Salt plates were prepared from 15 g Seakem LE agarose (BMA), 2.1 g free arginine base (Sigma), 1 ml 1 M $MgSO_4$, 100 µl 1 M CaCl2, 1.5 g dropout powder, 20 g dextrose, 2 ml 500x trace minerals (Q Biogene), 1 ml 1000x vitamins (7) in 1 liter water and adjusted to pH 6.0 with phosphoric acid. KCl was added to 100 mM or 0.5 mM.

Yeast Screen

A subset of the yeast deletion library (1) consisting of 376 yeast strains (online Table S1) each carrying a deletion in an early secretory pathway-localized protein (8) was mated to yeast expressing Kir3.2S177W-GFP using a modified version of the method for Synthetic Genetic Array analysis (9). The selection scheme is shown online in Table S2. After sporulation, strains were plated in triplicate. Growth of the double mutant strains was tested on synthetic media containing 750 mM NaCl and dextrose or galactose, to repress or induce channel expression, respectively. Growth tests were performed in duplicate (diagonally pinned) for each of the triplicates. Plates were photographed using a ChemiImager Ready (Alpha Innotech Corp.) and colony sizes, S_{gal} and S_{dex}, measured using software developed by Collins *et al*. (10). Colony sizes were analyzed by calculating the difference in size of each colony on galactose versus dextrose (S_{gal}*100/S_{dex} – 100). Initial Na^+-tolerant candidates had to meet the criterion that four out of six replicates or the average of the six colony size differences |S_{gal}*100/S_{dex} – 100| were smaller than the average |S_{gal}*100/S_{dex} – 100| for all strains tested minus one standard deviation.

Yeast Media for screen

Yeast media was prepared according to (9). For tests on high Na^+, the following media was prepared analogously to the procedures for single mutant and double mutant selection plates described in (9):

Na test: 750mM Na SD(MSG) -HIS-ARG-LYS-URA +CAN+S-AEC+G418 +citrate

agar [g]	20
water [ml]	700

YNB -aa -(NH4)SO4 [g]	1.7
aa -HIS-ARG-LYS-URA [g]	2
MSG [g]	1
40% dextrose [ml]	50
water [ml]	250
100mg/ml canavanine [ml]	0.5
100mg/ml S-AEC [ml]	0.5
50mg/ml geneticin [ml]	4
Na_3 citrate [g]	5.9
NaCl [g]	40.3

pH7 with 1M Tris

Na test: 750mM Na SGR(MSG) -HIS-ARG-LYS-URA +CAN+S-AEC+G418 +citrate

agar [g]	20
water [ml]	700

YNB -aa -(NH4)SO4 [g]	1.7
aa -HIS-ARG-LYS-URA [g]	2
MSG [g]	1
20% galactose [ml]	100
20% raffinose [ml]	100
water [ml]	100
100mg/ml canavanine [ml]	0.5
100mg/ml S-AEC [ml]	0.5
50mg/ml geneticin [ml]	4
Na_3 citrate [g]	5.9
NaCl [g]	40.3

pH7 with 1M Tris

Barium test

Wildtype yeast with or without a genomic insertion of Kir* were plated in a lawn on 500 mM NaCl YPAGR media. Filter disks (Whatman, 1cm diameter) soaked in 100 μl water or 100 μl 100 mM $BaCl_2$ were placed on the lawns as described in (11). Photographs were taken two or three days after plating.

Growth assays

Doubling times and growth rates were determined at 30°C by diluting over night cultures to about $2 * 10^6$ cells/ml into 2 ml media, allowing the cells to adjust for one hour before measuring the 0 hour (t0) optical density (OD) at 660nm in a spectrophotometer (Ultrospec 21000 Pro, Amersham). The second time point (t1) was measured 4h (for YPAGR) or 8h (for 500mM NaCl YPAGR, 500mM NaCl YPAD, 500 mM NaCl YPAGR with 500 mg/l hygromycin) later. Optical densities were converted to cell numbers (N) based on the polynomial

$$N\ [\text{cells/ml}] = 0.0219 + 1.3223 * OD - 0.601 * OD^2 + 1.1309 * OD^3$$

fitted to the table published by (12). Doubling times were calculated based on (12):

$$t_{double} = (t1-t0) * \ln 2 / \ln(N_{t1}/N_{t0})$$

Relative growth rates with versus without hygromycin were calculated as:

relative growth rate with hygromycin/no hygromycin

$= t_{double}$ without hygromycin / t_{double} with hygromycin

(growth rate = $\ln 2 / t_{double}$).

For dilutions on rich media, over night cultures grown in YPAD or YPAGR were diluted to $2 * 10^5$, $2 * 10^4$, and $2 * 10^3$ cells/ml in water and 2.5 µl drops spotted onto agar plates. For dilutions on Low Salt plates, over night cultures grown in 100 mM KCl SD-MET media were diluted to 10^6, 10^5, and 10^4 cells/ml in 25% glycerol and 10 µl drops spotted onto agar plates. 25% glycerol was used to overcome the high surface tension of water on low salt plates, which caused the cells to clump at the center of the drops as the water evaporated. Photographs were taken three days after plating.

Western sample preparation

Yeast protein samples were prepared by the post-alkaline lysis method (13). Briefly, $2 * 10^7$ cells from an over night culture grown in YPAGR were pelleted at 1,000 g for 1 minute and resuspended in 100 µl water. 100 µl 0.2 M NaOH was added and the cells incubated for 4 minutes at RT, followed by pelleting for 1 min at 1,000 g and resuspension in 200 µl sample buffer (60 mM TrisHCl pH6.8, 2% SDS, 10% glycerol, 0.0025% bromophenol blue, 4% β-mercaptoethanol), and heating to 95°C for 3 minutes. Proteins were separated on 10% Bis-tris gels in MOPS running buffer (Invitrogen) with antioxidant (Invitrogen) in the upper chamber or on 10% Tris-glycine gels (BioRad) in Tris-glycine buffer and transferred in Tris-glycine-methanol buffer to PVDF membrane (Millipore). Membranes were blocked with 3% milk and probed with rabbit anti-GIRK2 1:1000 (Alomone), mouse anti-PGK 1:1000 (Molecular Probes), or rabbit anti-Gas1p 1:2500 (Walter lab) antibodies. Binding of HRP conjugated secondary antibodies 1:10,000 (Jackson Immuno) was detected using Pico ECL substrate (Pierce) and captured on film (Denville).

Imaging

Yeast strains were grown for 12 h in SGR media supplemented with adenine, fixed by addition of 8% methanol-free formaldehyde (Polysciences) in 2x PBS for 1 h at RT, washed once with PBS, and mounted in DAPI containing Prolong Gold antifade (Molecular Probes). Imaging was performed with a widefield epifluorescence Exfo X-Cite 120 source connected to a Nikon TE2000 inverted microscope using a CFI Plan

Apochromat TIRF 100x objective (NA 1.49) and Photometrics CoolSnap HQ2 camera. Optical z stacks (100 nm thickness, 47 planes, 300 ms exposure per plane) were acquired using Nikon Elements AR 2.30 imaging software. Stacks were deconvolved with 3D blind deconvolution algorithms using MediaCybernetics AutoDeblur X1.4.1. Images presented are single planes from the middle and top of deconvolved stacks. A single image of DAPI fluorescence at the center of the cells was acquired (not shown).

Unfolded protein response assay

The YMS612 strain contains a genomically integrated reporter construct consisting of four repeats of the Unfolded Protein Response Element (UPRE) upstream of GFP immediately followed by mCherry RFP driven from a TEF2 promoter. The mCherry served as a normalization reference to compensate for changes in cell fluorescence due to cell growth rates and abnormal size distributions that were unrelated to UPR induction. Single mutants expressing the reporter were made by mating YMS612 with strains taken from the MATa KAN^r yeast deletion library (1). Diploids were made using a NAT^r cassette.

Strains were inoculated in 25μl YEPD and allowed to saturate overnight in a 384 well plate at 30°C without shaking. They were observed to reach OD_{600}=8-9. Cultures were back-diluted to OD=0.08-0.09, incubated for 4.5-5.5 h until they reached OD=0.3-0.6 and injected into a Becton Dickinson LSRII flow cytometer using a high throughput sampler (14). The normalized GFP/RFP fluorescence ratio for each sample was obtained by taking the median of the GFP to RFP ratios of all events in a sample. The reported values represent means of the GFP/RFP fluorescence ratio of at least two measurements. Error bars represent standard error of the mean.

References

1. Giaever, G. & others (2002) *Nature* 418, 387-91.
2. Brachmann, C. B., Davies, A., Cost, G. J., Caputo, E., Li, J., Hieter, P. & Boeke, J. D. (1998) *Yeast* 14, 115-32.
3. Yi, B. A., Lin, Y. F., Jan, Y. N. & Jan, L. Y. (2001) *Neuron* 29, 657-67.
4. Bichet, D., Lin, Y. F., Ibarra, C. A., Huang, C. S., Yi, B. A., Jan, Y. N. & Jan, L. Y. (2004) *Proc Natl Acad Sci U S A* 101, 4441-6.
5. Minor, D. L., Jr., Masseling, S. J., Jan, Y. N. & Jan, L. Y. (1999) *Cell* 96, 879-91.
6. Treco, D. A. & Lundblad, V. (1993) *Current Protocols in Molecular Biolog, 13.1.1-13.1.7.*
7. Nakamura, R. L. & Gaber, R. F. (1998) *Methods Enzymol* 293, 89-104.
8. Schuldiner, M., Collins, S. R., Thompson, N. J., Denic, V., Bhamidipati, A., Punna, T., Ihmels, J., Andrews, B., Boone, C., Greenblatt, J. F., Weissman, J. S. & Krogan, N. J. (2005) *Cell* 123, 507-19.
9. Schuldiner, M., Collins, S. R., Weissman, J. S. & Krogan, N. J. (2006) *Methods* 40, 344-52.
10. Collins, S. R., Schuldiner, M., Krogan, N. J. & Weissman, J. S. (2006) *Genome Biol* 7, R63.
11. Chatelain, F. C., Alagem, N., Xu, Q., Pancaroglu, R., Reuveny, E. & Minor, D. L., Jr. (2005) *Neuron* 47, 833-43.

12. Amberg, D. C., Burke, D. J. & Strathern, J. N. (2005) *Methods in Yeast Genetics* (Cold Spring Harbor Laboratory Press, Cold Spring Harbor, NY, USA).
13. Kushnirov, V. V. (2000) *Yeast* 16, 857-60.
14. Newman, J. R., Ghaemmaghami, S., Ihmels, J., Breslow, D. K., Noble, M., DeRisi, J. L. & Weissman, J. S. (2006) *Nature* 441, 840-6.